

Milling Processes and Hydrogen Storage Properties of Mg-Graphene Composites

Young Jun KWAK¹, Eunho CHOI², Myoung Youp SONG^{1,*}

¹Division of Advanced Materials Engineering, Hydrogen & Fuel Cell Research Center, Engineering Research Institute, Chonbuk National University, 567 Baekje-daero Deokjin-gu Jeonju, 54896, Republic of Korea

²Department of Materials Engineering, Graduate School, Chonbuk National University, 567 Baekje-daero Deokjin-gu Jeonju, 54896, Republic of Korea

crossref <http://dx.doi.org/10.5755/j01.ms.25.3.20567>

Received 13 April 2018; accepted 16 July 2018

Graphene was chosen as an additive to improve the hydrogen uptake and release properties of magnesium (Mg). Five weight percent of graphene was added to Mg or pre-milled Mg by milling in hydrogen (reactive milling). The milling processes and hydrogen uptake and release properties of the graphene-added Mg were investigated. Adding graphene to Mg and then milling the mixture of Mg and graphene in hydrogen for 6 h [named M5G (6 h)] had little effects on the improvement of hydrogen uptake and release properties of Mg. Pre-milling of Mg (for 24 h) and then adding 5 wt.% of graphene by milling in hydrogen (for 30 min) (named M5G) significantly increased the hydrogen uptake and release rates and the quantities of hydrogen absorbed and released for 60 min of Mg. The activation of M5G was completed after cycle number, CN, of two (CN = 2). M5G had a high effective hydrogen-storage capacity of 6.21 wt.% at 623 K in 12 bar H₂ at CN = 3. M5G released 0.25 wt.% hydrogen for 2.5 min and 5.28 wt.% hydrogen for 60 min H₂ in 1.0 bar H₂ at 623 K at CN = 3. Pre-milling of Mg and then adding graphene by milling in hydrogen and hydrogen uptake-release cycling are believed to create defects, produce cracks and clean surfaces, and decrease particle sizes.

Keywords: hydrogen storage materials, milling in hydrogen, hydrogen uptake and release rates, microstructure, graphene-added Mg alloy.

1. INTRODUCTION

Magnesium (Mg) is known to have excellent hydrogen-storage properties, except that it has low hydrogen uptake and release rates. To increase the hydrogen uptake and release rates of Mg, transition metals like Pd [1], Cu [2], Co, Ni or Fe [3, 4], and Ti [5], rare-earth metals such as La and Y [6], graphite [7, 8], or intermetallic compounds such as Mg₂Ni, LaNi₅, and FeTi [9–11] have been added to Mg.

Of the studies in which carbon materials have been doped, Huot et al. [7] synthesized a metallic hydride rapidly by milling Mg with graphite at a high temperature under hydrogen pressure. They were able to form hydride by milling a mixture of Mg + 5 at% V + graphite at 573 K under 4 bar H₂ for 1 h. Popilevsky et al. [8] synthesized pelletized porous composites of Mg admixed with 2 wt.% of either multiwall carbon nanotubes or graphite. They reported that the best combination of hydrogen desorption kinetics, thermal conductivity, and mechanical stability was obtained for the pellets synthesized from the mixture of Mg with 2 wt.% of carbon nanotubes processed by 4 h of co-milling [8]. Imamura et al. [12] obtained nanocomposites by mechanically milling Mg, graphite, and organic additive (benzene, cyclohexene or cyclohexane). In the obtained nanocomposites, many dangling carbon bonds were formed in the graphite due to the decomposition of the graphite structure, which was caused by mechanical milling. The hydrogen absorbed in these

nanocomposites existed as a C-H bond type in graphite and as hydride type in Mg.

Graphite has a high thermal conductivity compared with most metals except gold, silver, copper, and aluminium. When graphite is added to Mg, it can thus help the sample have higher hydrogen uptake and release rates by dispersing heat rapidly. The average specific gravity of graphite is 1.6–2.0, which is smaller than the specific gravity of aluminium, and the specific surface area of graphite is large.

In the present work, graphene was chosen as an additive to improve the hydrogen uptake and release properties of Mg. Five weight percent of graphene was added to Mg or pre-milled Mg by milling in hydrogen (reactive milling). The milling processes and hydrogen uptake and release properties of the graphene-added Mg (named M5G) were investigated.

2. EXPERIMENTAL DETAILS

Pure Mg powder (–20 + 100 mesh, 99.8 %, metals basis, Alfa Aesar) and graphene (3–10 multi-layer graphene, 5–10 μm, purity ≥ 99 wt.%, thickness nanometer 3–6 nm, surface area 150 m²/g, chemical exfoliation proprietary method, Carbon Nano-material Technology Co., LTD) were used as starting materials.

Reactive milling refers to the milling of a material in a reactive gas atmosphere and in this work, the reactive milling was performed in a hydrogen atmosphere. In the present work, milling in hydrogen to obtain the final samples is referred to as reactive milling and milling in hydrogen before reactive milling to obtain the final samples is referred to as pre-milling.

* Corresponding author. Tel.: +82-63-270-2379; fax: +82-63-270-2386
E-mail address: songmy@jbnu.ac.kr (M.Y. Song)

Reactive milling to prepare a M5G (6 h) sample, which has a composition of 95 wt.% (Mg without pre-milling) + 5 wt.% graphene, was performed in a planetary ball mill (Planetary Mono Mill; Pulverisette 6, Fritsch). Samples with the desired compositions (total weight = 8 g) were mixed in a hermetically sealed stainless steel container with 105 hardened steel balls (total weight = 360 g); the sample to ball weight ratio was 1/45. All sample handling was performed in a glove box under Ar in order to prevent oxidation. The disc revolution speed was 400 rpm. The mill container (volume of 250 mL) was then filled with high purity hydrogen gas (~ 12 bar). Milling was performed for 6 h, during which the mill container was refilled with hydrogen every two hours.

Pre-milling of Mg was performed under the conditions similar to those for the preparation of M5G (6 h). Pre-milling of Mg was performed for 24 h.

To prepare M5G, which was prepared using pre-milled Mg, the addition of graphene was also performed in a planetary ball mill (Planetary Mono Mill; Pulverisette 6, Fritsch). 95 wt.% (Mg pre-milled for 24 h) + 5 wt.% graphene (total weight = 8 g) were mixed under the conditions similar to those for the preparation of M5G (6 h). Reactive milling to prepare M5G was performed for 30 min.

Table 1 shows the names, compositions, and preparation conditions of the prepared samples.

The absorbed or released hydrogen quantity was measured as a function of time in nearly constant hydrogen pressures (in 12 bar H₂ for hydrogen uptake and in 1.0 bar H₂ for hydrogen release) using the volumetric method, with the Sieverts' type hydrogen uptake and release apparatus described previously [13]. 0.5 g of the samples was used for these measurements.

Samples after reactive milling and after hydrogen uptake-release cycling were characterized by X-ray diffraction (XRD) with Cu K α radiation, using a Rigaku D/MAX 2500 powder diffractometer. The microstructures of the powders were observed using a JSM-5900 scanning electron microscope (SEM) operated at 20 kV. Raman spectrum measurements were done with an NTEGRA (NT-MDT, Russia) Raman microscope with a laser excitation wavelength of 532 nm.

Table 1. Names, compositions, and preparation conditions of the prepared samples

Sample names	Compositions	Pre-milling time of Mg in H ₂ , h	Milling in H ₂
M5G (6 h)	95 wt% Mg + 5 wt% graphene	0	6 h
M5G	95 wt% Mg + 5 wt% graphene	24	30 min with graphene

3. RESULTS AND DISCUSSION

Graphene is an allotrope of carbon and consists of a single layer of carbon atoms arranged in a hexagonal lattice. Fig. 1 shows the XRD pattern of graphene, with the Miller indices of the faces marked.

The SEM micrographs of graphene at different magnifications are shown in Fig. 2. Particle sizes were not homogeneous; some particles were very large and some

were fine.

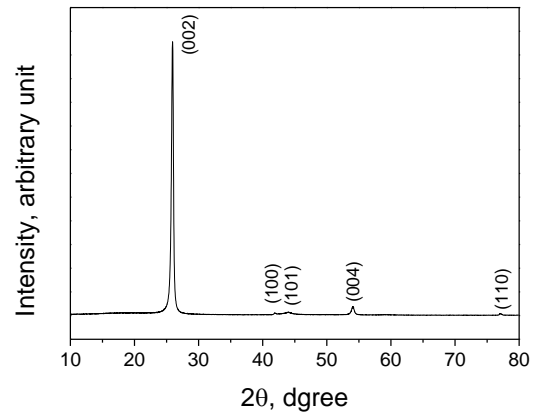


Fig. 1. XRD pattern of graphene

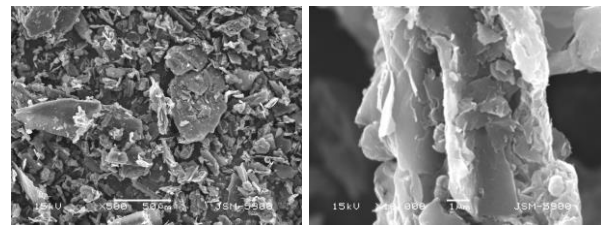


Fig. 2. SEM micrographs of graphene at different magnifications

The shapes of particles were very irregular; some particles were flat and some were rod-like. The average particle size was obtained by linear intercept technique [14]. The average particle size of the graphene was 14.1 μm .

Raman spectra of the graphene and as-prepared M5G are shown in Fig. 3. Raman spectrum measurements were done with a laser excitation wavelength of 532 nm. The Raman spectrum of the graphene used in this work exhibited D, G, and 2D peaks, which can be assigned to graphene. The Raman shifts of the D, G, and 2D peaks for graphene were 1355, 1584, and 2713 cm^{-1} , respectively. The ratio of intensities of the D and G peaks, I_D/I_G , for graphene was 0.809. Ferrari et al. [15] reported that the shape and intensity of the 2D peak of graphene changed significantly compared with bulk graphite and the 2D peak of bulk graphite consists of two components 2D₁ and 2D₂. Ferrari et al. also reported that the graphene D peak is a single sharp peak, while in graphite it is a band consisting of two peaks, D₁ and D₂ [15]. The Raman spectrum in Fig. 3 shows that the material used in this work was not graphite but graphene. It was reported that I_G/I_{2D} is about 0.3 in single-layer and increases linearly until quintuple layers, and saturated in more than sextuple layers [16]. The graphene used in this work (Fig. 2 a) had I_G/I_{2D} of 1.77, showing that the graphene used in this work was multilayer graphene. Hodkiewicz et al [17] reported that the D peak is known as the disorder band or the defect band and the intensity of the D peak is directly proportional to the level of defects in the sample. Rusi & S. R. Majid [18] reported that increments of I_D/I_G can be attributed to an increase in defects on the surface of the sample that were induced during the synthesis process. The ratio of intensities of D and G peaks, I_D/I_G , for as-prepared M5G was 1.321. The increase in I_D/I_G after reaction-involving milling of the pre-milled Mg with graphene shows that defects and disordering

in the graphene were increased. As formation of the defects in graphene, we can consider the formation of point defects (vacancies) in the lattice points of the hexagonal basal plane. For disordering, we can consider the formation of stacking fault disorder and turbostratic graphite. In the graphene, stacking fault disorder is known to be generated due to forward shearing of the hexagonal basal planes after mechanical milling [19]. The turbostratic graphite is the graphene which has curled, twisted, and rotated planes [19]. Rather than the former (the formation of defects in graphene) since high energy is considered to be required to make vacancies in the lattice points of the hexagonal basal plane, we believe that, the latter (the generation of stacking fault disorder and the formation of turbostratic graphite) occurred after milling with the pre-milled Mg.

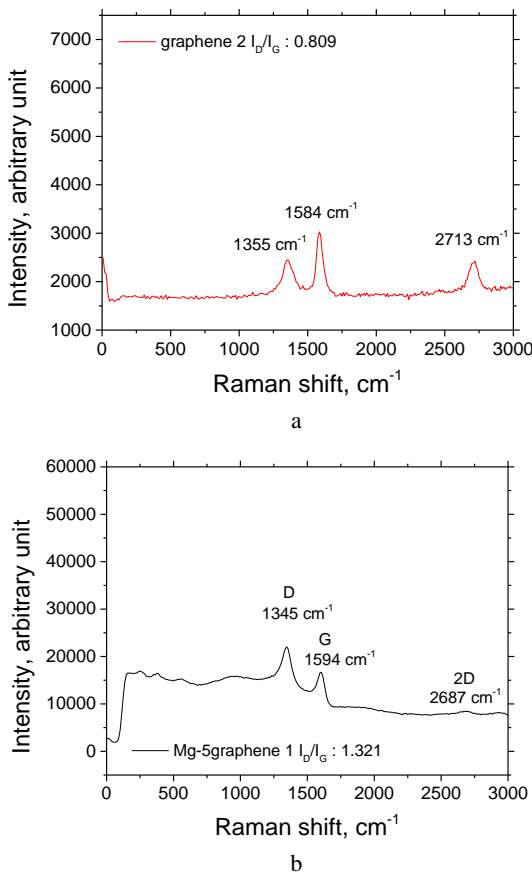


Fig. 3. Raman spectra: a – graphene; b – as-prepared M5G

The quantity of hydrogen absorbed by the sample, U , was defined with respect to the sample weight. The quantity of hydrogen released by the sample, R , was also defined with respect to the sample weight. U and R were expressed in the unit of wt.% hydrogen.

Fig. 4 shows the variation in the U versus time t curve in 12 bar H_2 with the cycle number, CN, and the R versus t curve in 1.0 bar H_2 at CN=1, at 593 K for M5G (6 h), which was prepared by milling a mixture of 95 wt.% Mg (not pre-milled) + 5 wt.% graphene for 6 h. From CN = 1 to CN = 4, the initial hydrogen uptake rate of M5G (6 h) was low and the quantity of hydrogen absorbed for 60 min, U (60 min), of M5G (6 h) was small. The initial hydrogen uptake rate and U (60 min) decreased from CN = 1 to CN = 3 and increased from CN = 3 to CN = 4. At CN = 1, M5G (6 h) absorbed 0.23 wt.% hydrogen for 2.5 min,

0.23 wt.% hydrogen for 10 min, and 0.37 wt.% hydrogen for 60 min. At CN = 4, M5G (6 h) absorbed 0.23 wt.% hydrogen for 2.5 min, 0.23 wt.% hydrogen for 10 min, and 0.27 wt.% hydrogen for 60 min. The R versus t curves were very similar from CN = 1 to CN = 4. From CN = 1 to CN = 4, the initial hydrogen release rate of M5G (6 h) was low and the quantity of hydrogen released for 60 min, R (60 min), of M5G (6 h) was small. At CN = 1, M5G (6 h) released 0.06 wt.% hydrogen for 2.5 min, 0.09 wt.% hydrogen for 10 min, and 0.13 wt.% hydrogen for 60 min.

We define an effective hydrogen-storage capacity as the quantity of hydrogen absorbed for 60 min. M5G (6 h) had a small effective hydrogen-storage capacity of 0.37 wt.% at 593 K in 12 bar H_2 at CN = 1.

The results in Fig. 4 show that adding graphene to Mg and then grinding the mixture of Mg and graphene in hydrogen has little effects on the improvement of the hydrogen uptake and release properties of Mg.

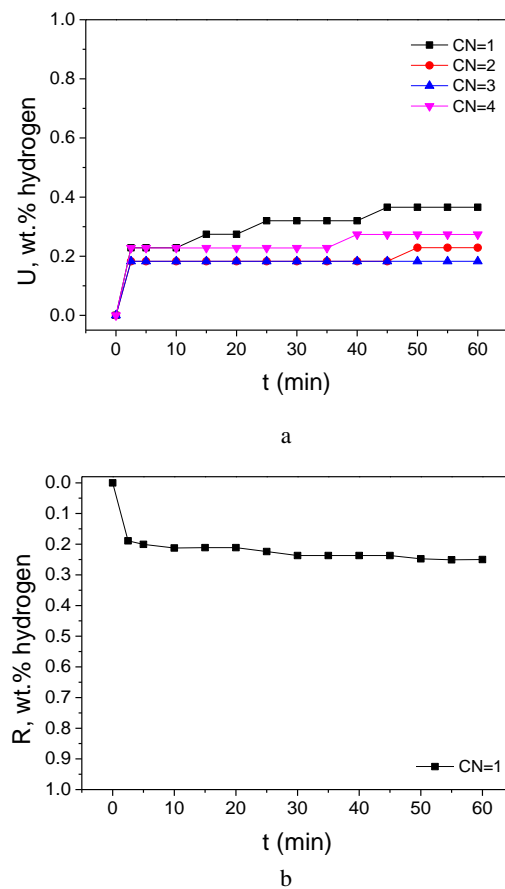


Fig. 4. a – variation in the U versus t curve in 12 bar H_2 with the cycle number, CN; b – the R versus t curve in 1.0 bar H_2 at CN=1, at 593 K for M5G (6 h)

Fig. 5 shows the variation in the U versus t curve with the cycle number at 573 K in 12 bar H_2 for M5G. At CN = 1, the initial hydrogen uptake rate of M5G was relatively high and the quantity of hydrogen absorbed for 60 min, U (60 min), was relatively large. As CN increased from one to three, the initial hydrogen uptake rate of M5G increased and from CN = 3 to CN = 4, the initial hydrogen uptake rate of M5G decreased. As CN increased from one to three, the U (60 min) of M5G decreased and from CN = 3 to CN = 4, the U (60 min) of M5G increased.

These results indicate that the activation of M5G was completed after CN = 2. At CN = 1, M5G absorbed 0.95 wt.% hydrogen for 2.5 min, 2.26 wt.% hydrogen for 10 min, and 5.55 wt.% hydrogen for 60 min. At CN = 3, M5G absorbed 1.82 wt.% hydrogen for 2.5 min, 3.28 wt.% hydrogen for 10 min, and 4.70 wt.% hydrogen for 60 min. Table 2 presents the variations of U with t at 573 K in 12 bar H_2 at CN = 1–4 for M5G.

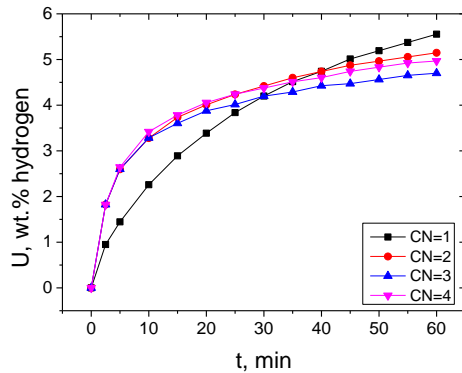


Fig. 5. Variations in the U versus t curve in 12 bar H_2 with the cycle number at 573 K for M5G

M5G had quite a high effective hydrogen-storage capacity of 5.55 wt.% at CN = 1 and a high effective hydrogen-storage capacity of 4.70 wt.% at CN = 3 at 593 K in 12 bar H_2 .

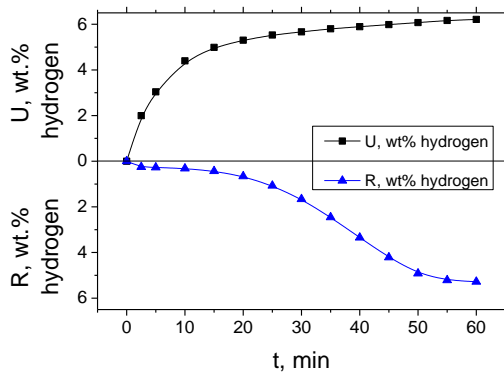


Fig. 6. U versus t curve in 12 bar H_2 and R versus t curve in 1.0 bar H_2 at 623 K at CN = 3 for M5G

The U versus t curve in 12 bar H_2 and R versus t curve in 1.0 bar H_2 at 623 K at CN = 3 for M5G are shown in Fig. 6. The initial hydrogen uptake rate of M5G was quite high and the U (60 min) of M5G was quite large. M5G absorbed 1.99 wt.% hydrogen for 2.5 min, 4.40 wt.% hydrogen for 10 min, and 6.21 wt.% hydrogen for 60 min. The R versus t curve exhibited momentary hydrogen release of 0.25 wt.% in the beginning. This is believed to result from the hydrogen desorbed from the surfaces of the particles and released from the MgH_2 -H solid solution. We believe that the hydrogen quantity from the MgH_2 -H solid solution is smaller than that from the surfaces of the particles since it has been reported that the quantity of hydrogen contained in the MgH_2 -H solid solution is small [20]. The R versus t curve was S-shaped, indicating that the hydrogen release reaction progressed by a nucleation and growth mechanism. The initial hydrogen release rate was

relatively low, and the hydrogen release rate was the highest in about 35 min. M5G released 0.25 wt.% hydrogen for 2.5 min, 0.32 wt.% hydrogen for 10 min, and 5.28 wt.% hydrogen for 60 min. Table 3 shows the variations of R with t in 1.0 bar H_2 and U with t in 12 bar H_2 at 623 K at CN = 3 for M5G.

Table 2. Variations of U (wt.% hydrogen) with t at 573 K in 12 bar H_2 at CN = 1–4 for M5G

	2.5 min	5 min	10 min	30 min	60 min
CN = 1	0.95	1.44	2.26	4.20	5.55
CN = 2	1.82	2.60	3.28	4.42	5.15
CN = 3	1.82	2.60	3.28	4.20	4.70
CN = 4	1.82	2.64	3.42	4.38	4.97

Table 3. Variations of R (wt.% hydrogen) with t in 1.0 bar H_2 and U with t in 12 bar H_2 at 623 K at CN = 3 for M5G

	2.5 min	5 min	10 min	30 min	60 min
U	1.99	3.04	4.40	5.67	6.21
R	0.25	0.27	0.32	1.66	5.28

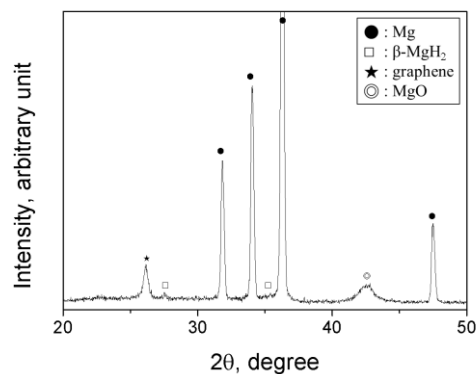


Fig. 7. XRD pattern of M5G dehydrogenated at the 4th hydrogen uptake-release cycle

Fig. 7 shows the XRD pattern of M5G dehydrogenated at the 4th hydrogen absorption-release cycle. The M5G after reactive milling contained a large amount of Mg and small amounts of β - MgH_2 and graphene. This shows that β - MgH_2 formed by the reaction of Mg with H_2 during milling in hydrogen. β - MgH_2 is a low pressure form of magnesium hydride with a tetragonal structure. The M5G dehydrogenated at the 4th hydrogen uptake-release cycle contained a large amount of Mg, a small amount of graphene, and very small amounts of β - MgH_2 and MgO. A very small amount of MgO is considered to be formed by the reaction of Mg with oxygen adsorbed on the particle surfaces during treating the samples to obtain the XRD pattern. The grain sizes of Mg and MgH_2 in the samples were calculated using Scherrer formula. The grain sizes of Mg and MgH_2 in the M5G after reactive milling were 25.8 nm and 17.9 nm, respectively. The grain sizes of Mg and MgH_2 in the M5G dehydrogenated at the 4th hydrogen uptake-release cycle were 30.9 nm and 56.9 nm, respectively. The grain size of Mg increased after hydrogen uptake-release cycling.

The SEM micrographs of M5G after reactive milling and M5G dehydrogenated at the 4th hydrogen uptake-release cycle is shown in Fig. 8. M5G after reactive milling had no homogeneous particle size and its particles had

some cracks and the particle surfaces were undulated. M5G dehydrogenated at the 4th hydrogen uptake-release cycle had a microstructure similar to that of M5G after reactive grinding. The average particle size of the M5G after reactive milling was 11.7 μm while that of the M5G dehydrogenated at the 4th hydrogen uptake-release cycle was 12.50 μm , indicating that these two samples had similar particle sizes. However, the particles of M5G dehydrogenated at the 4th hydrogen uptake-release cycle had more cracks than those of M5G after reactive milling. The particles of M5G dehydrogenated at the 4th hydrogen uptake-release cycle had some fine particles on their surfaces. The formation of cracks and fine particles with hydrogen uptake-release cycling are considered to result from the expansion and contraction of Mg with hydrogen uptake-release cycling.

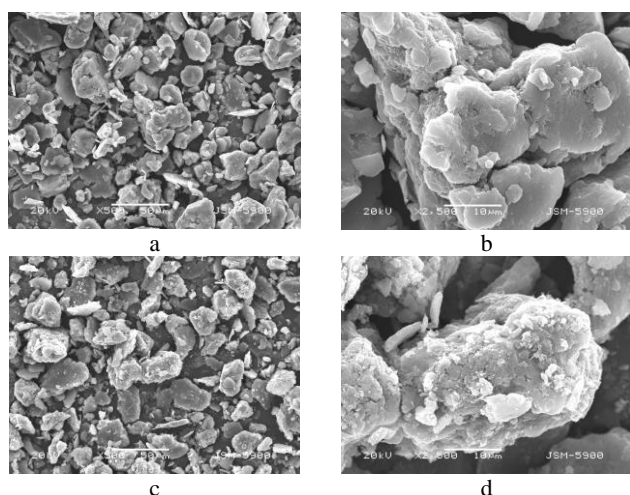


Fig. 8. SEM micrographs of M5G: a, b—after reactive milling; c, d—dehydrogenated at the 4th hydrogen uptake-release cycle

Fig. 5 shows that from CN = 1 to CN = 3, the initial hydrogen uptake rate of M5G increased and the U (60 min) of M5G decreased. It is believed that from CN = 1 to CN = 3, the initial hydrogen uptake rate of M5G increased due to formation cracks on the surfaces of particles from expansion and contraction of the particles and the U (60 min) of M5G decreased due to coalescence of cracks inside particles.

M5G (6 h), which was prepared by reactive milling without pre-milling Mg, has a low initial hydrogen uptake rate and a small U (60 min). It is considered that acting of the added graphene as a lubricant hindered the pulverization of Mg. To pulverize Mg particles, they were milled in hydrogen for relatively long times (24 h). Pre-milling of Mg and then adding graphene by milling in hydrogen significantly increased the initial hydrogen uptake rate and the U (60 min) of Mg.

Pre-milling of Mg is believed to create defects (leading to facilitation of nucleation), produce cracks and clean surfaces (leading to increase in reactivity), and decrease particle sizes (leading to diminution of diffusion distances or increasing the flux of the diffusing hydrogen atoms). Adding graphene, which has a large specific surface area, to the pre-milled Mg is believed to decrease particle sizes by graphene's filling the cracks of Mg particles and helping the Mg particles be separated [21–24].

The hydrogen uptake-release cycling is also believed to create defects, produce cracks and clean surfaces, and decrease particle sizes due to expansion (by hydrogen uptake) and contraction (by hydrogen release) of Mg [25–28].

4. CONCLUSIONS

Adding graphene to Mg and then milling the mixture of Mg and graphene in hydrogen for 6 h (named M5G (6 h)) had little effects on the improvement of hydrogen uptake and release properties of Mg. Pre-milling of Mg (for 24 h) and then adding graphene by milling in hydrogen (for 30 min) (named M5G) significantly increased the hydrogen uptake and release rates and the quantities of hydrogen absorbed and released for 60 min of Mg. The activation of M5G was completed after cycle number, CN, of two (CN = 2). M5G had a high effective hydrogen-storage capacity of 6.21 wt.% at 623 K in 12 bar H_2 at CN = 3. M5G released 0.25 wt.% hydrogen for 2.5 min and 5.28 wt.% hydrogen for 60 min H_2 in 1.0 bar H_2 at 623 K at CN = 3. Pre-milling of Mg and then adding graphene are believed to create defects, produce cracks and clean surfaces, and decrease particle sizes. The hydrogen uptake-release cycling is believed to bring about similar effects.

Acknowledgements

This research was supported by Basic Science Research Program through the National Research Foundation of Korea (NRF) funded by the Ministry of Education (grant number NRF-2017R1D1A1B03030515).

REFERENCES

1. **Krozer, A., Kasemo, B.** Equilibrium Hydrogen Uptake and Associated Kinetics for the Mg- H_2 System at Low Pressures *Journal of Physics: Condensed Matter* 1 (8) 1989: pp. 1533–1538. <https://doi.org/10.1088/0953-8984/1/8/017>
2. **Karty, A., Genossar, J.G., Rudman, P.S.** Hydriding and Dehydriding Kinetics of Mg in a Mg/Mg₂Cu Eutectic Alloy: Pressure Sweep Method *Journal of Applied Physics* 50 (11) 1979: pp. 7200–7209. <https://doi.org/10.1063/1.325832>
3. **Bobet, J.L., Akiba, E., Nakamura, Y., Darriet, B.** Study of Mg-M (M=Co, Ni and Fe) Mixture Elaborated by Reactive Mechanical Alloying-Hydrogen Sorption Properties *International Journal of Hydrogen Energy* 25 (10) 2000: pp. 987–996. [https://doi.org/10.1016/S0360-3199\(00\)00002-1](https://doi.org/10.1016/S0360-3199(00)00002-1)
4. **Reilly, J.J., Wiswall, R.H.** Reaction of Hydrogen with Alloys of Magnesium and Copper *Inorganic Chemistry* 7 (11) 1968: pp. 2254–2256. <https://doi.org/10.1021/ic50069a016>
5. **Calizzi, M., Chericoni, D., Jepsen, L.H., Jensen, T.R., Pasquini, L.** Mg-Ti Nanoparticles with Superior Kinetics for Hydrogen Storage *International Journal of Hydrogen Energy* 41 (32) 2016: pp. 14447–14454. <https://doi.org/10.1016/j.ijhydene.2016.03.071>
6. **Tran, N.E., Imam, M.A., Feng, C.R.** Evaluation of Hydrogen Storage Characteristics of Magnesium-Misch

- Metal Alloys *Journal of Alloys Compounds* 359 (1–2) 2003: pp. 225–229.
[https://doi.org/10.1016/S0925-8388\(03\)00176-2](https://doi.org/10.1016/S0925-8388(03)00176-2)
7. **Huot, J., Tremblay, M.L., Schulz, R.** Synthesis of Nanocrystalline Hydrogen Storage Materials *Journal of Alloys Compounds* 356–357 2003: pp. 603–607.
[https://doi.org/10.1016/S0925-8388\(03\)00120-8](https://doi.org/10.1016/S0925-8388(03)00120-8)
 8. **Popilevsky, L., Skripnyuk, V.M., Beregovsky, M., Senzen, M., Amouyal, Y., Rabkin, E.** Hydrogen Storage and Thermal Transport Properties of Pelletized Porous Mg-2 wt.% Multiwall Carbon Nanotubes and Mg-2 wt.% Graphite Composites *International Journal of Hydrogen Energy* 41 (32) 2016: pp. 14461–14474.
<https://doi.org/10.1016/j.ijhydene.2016.03.014>
 9. **Guoxian, L., Erde, W., Shoushi, F.** Hydrogen Absorption and Desorption Characteristics of Mechanically Milled Mg-35 wt.% FeTi_{1.2} Powders *Journal of Alloys Compounds* 223 (1) 1995: pp. 111–114.
[https://doi.org/10.1016/0925-8388\(94\)01465-5](https://doi.org/10.1016/0925-8388(94)01465-5)
 10. **Liang, G., Boily, S., Huot, J., Neste, A.V., Schulz, R.** Hydrogen Absorption Properties of a Mechanically Milled Mg–50 wt.% LaNi₅ Composite *Journal of Alloys Compounds* 268 (1–2) 1998: pp. 302–307.
[https://doi.org/10.1016/S0925-8388\(97\)00607-5](https://doi.org/10.1016/S0925-8388(97)00607-5)
 11. **Khrussanova, M., Bobet, J.L., Terzieva, M., Chevalier, B., Radev, D., Peshev, P., Darriet, B.** Hydrogen Storage Characteristics of Magnesium Mechanically Alloyed with YNi_{5–x}Al_x (x = 0, 1 and 3) Intermetallics *Journal of Alloys Compounds* 307 (1–2) 2000: pp. 283–289.
[https://doi.org/10.1016/S0925-8388\(00\)00842-2](https://doi.org/10.1016/S0925-8388(00)00842-2)
 12. **Imamura, H., Kusuhara, M., Minami, S., Matsumoto, M., Masanari, K., Sakata, Y., Itoh, K., Fukunaga, T.** Carbon Nanocomposites Synthesized by High-Energy Mechanical Milling of Graphite and Magnesium for Hydrogen Storage *Acta Materialia* 51 (20) 2003: pp. 6407–6414.
<https://doi.org/10.1016/j.actamat.2003.08.010>
 13. **Song, M.Y., Baek, S.H., Bobet, J.L., Song, J., Hong, S.H.** Hydrogen Storage Properties of a Mg-Ni-Fe Mixture Prepared via Planetary Ball Milling in a H₂ Atmosphere *International Journal of Hydrogen Energy* 35 (19) 2010: pp. 10366–10372.
<https://doi.org/10.1016/j.ijhydene.2010.07.161>
 14. **Kingery, W.D., Bowen, H.K., Uhlmann, D.R.** Introduction to Ceramics, 2nd edition, A Wiley-Interscience Publication, John Wiley & Sons New York, 1976: p. 728.
<https://trove.nla.gov.au/version/45656624>
 15. **Ferrari, A.C., Meyer, J.C., Scardaci, V., Casiraghi, C., Lazzeri, M., Mauri, F., Piscanec, S., Jiang, D., Novoselov, K.S., Roth, S., Geim, A.K.** Raman Spectrum of Graphene and Graphene Layers *Physical Review Letters* 97 2006: pp. 187401.
<https://doi.org/10.1103/PhysRevLett.97.187401>
 16. <https://www.nanophoton.net/applications/22.html>
 17. <https://tools.thermofisher.com/content/sfs/brochures/D19505~.pdf>
 18. **Rusi., Majid, S.R.** Green Synthesis of In Situ Electrodeposited rGO/MnO₂ Nanocomposite for High Energy Density Supercapacitors *Scientific Reports* 5 2015: Article number: 16195.
<https://doi.org/10.1038/srep16195>
 19. **Varin, R.A., Czujko, T., Wronski, Z.S.** Nanomaterials for Solid State Hydrogen Storage, Springer, 2009: pp. 301–302.
<https://doi.org/10.1007/978-0-387-77712-2>
 20. **Stampfer, J.F.Jr., Holley, C.E.Jr., Suttle, J.F.** The Magnesium-Hydrogen System *American Chemical Society* 82 (14) 1959: pp. 3504–3508.
<https://doi.org/10.1021/ja01499a006>
 21. **Park, H.R., Kwak, Y.J., Song, M.Y.** Increase in the Hydrogen-Sorption Rates and Hydrogen-Storage Capacity of MgH₂ by Adding a Small Proportion of Zn(BH₄)₂ *Korean Journal of Metals and Materials* 55 (9) 2017: pp. 656–662.
<https://doi.org/10.3365/KJMM.2017.55.9.657>
 22. **Hong, S.H., Kwak, Y.J., Song, M.Y.** Enhancement of the Hydrogen-Storage Characteristics of Mg by Adding Mg₂Ni and Ni to MgH₂ via High Energy Ball Milling in Hydrogen Atmosphere *Korean Journal of Metals and materials* 56 (1) 2018: pp. 59–65.
<https://doi.org/10.3365/KJMM.2018.56.1.59>
 23. **Hong, S.H., Song, M.Y.** Hydrogen Absorption and Release Properties of MgH₂, Mg₂Ni, and Ni-added Mg via Reactive Mechanical Grinding *Korean Journal of Metals and Materials* 56 (2) 2018: pp. 155–162.
<https://doi.org/10.3365/KJMM.2018.56.2.155>
 24. **Song, M.Y., Kwak, Y.J.** Comparison of the Hydrogen Release Properties of Zn(BH₄)₂-Added MgH₂ Alloy and Zn(BH₄)₂ and Ni-added MgH₂ Alloy *Korean Journal of Metals and Materials* 56 (3) 2018: pp. 244–251.
<https://doi.org/10.3365/KJMM.2018.56.3.244>
 25. **Kwak, Y.J., Park, H.R., Song, M.Y.** Advancement in the Hydrogen Absorbing and Releasing Kinetics of MgH₂ by Mixing with Small Percentages of Zn(BH₄)₂ and Ni *Metals and Materials International* 22 (2) 2018: pp. 423–432.
<https://doi.org/10.1007/s12540-018-0036-4>
 26. **Song, M.Y., Choi, E., Kwak, Y.J.** Development of a Mg-Based Alloy with a Hydrogen-Storage Capacity of 7 wt% by Adding a Polymer CMC via Transformation-Involving Milling *Korean Journal of Metals and Materials* 56 (5) 2018: pp. 392–399.
<https://doi.org/10.3365/KJMM.2018.56.5.392>
 27. **Song, M.Y., Kwak, Y.J.** Hydrogen uptake and release characteristics of Mg-xTaF₅-xVCl₃ (x = 1.25, 2.5, and 5) *Korean Journal of Metals and Materials* 56 (8) 2018: pp. 611–619.
<https://doi.org/10.3365/KJMM.2018.56.8.611>
 28. **Song, M.Y., Choi, E., Kwak, Y.J.** Raising the Dehydrogenation Rate of a Mg-CMC (Carboxymethylcellulose, Sodium Salt) Composite by Alloying Ni via Hydride-Forming Milling *Korean Journal of Metals and Materials* 56 (8) 2018: pp. 620–627.
<https://doi.org/10.3365/KJMM.2018.56.8.620>